

Dalton Transactions

Accepted Manuscript



This is an *Accepted Manuscript*, which has been through the Royal Society of Chemistry peer review process and has been accepted for publication.

Accepted Manuscripts are published online shortly after acceptance, before technical editing, formatting and proof reading. Using this free service, authors can make their results available to the community, in citable form, before we publish the edited article. We will replace this *Accepted Manuscript* with the edited and formatted *Advance Article* as soon as it is available.

You can find more information about *Accepted Manuscripts* in the [Information for Authors](#).

Please note that technical editing may introduce minor changes to the text and/or graphics, which may alter content. The journal's standard [Terms & Conditions](#) and the [Ethical guidelines](#) still apply. In no event shall the Royal Society of Chemistry be held responsible for any errors or omissions in this *Accepted Manuscript* or any consequences arising from the use of any information it contains.



ARTICLE

Preorganized tridentate analogues of mixed hydroxyoxime/carboxylate nickel extractants

James W Roebuck,^a Jennifer R Turkington,^a David M Rogers,^a Philip J Bailey,^a Violina Griffin,^b Adam J Fischmann,^b Gary S Nichol,^a Max Pelsler,^c Simon Parsons^a and Peter A Tasker^{a†}

Received 00th January 20xx,
Accepted 00th January 20xx

DOI: 10.1039/x0xx00000x

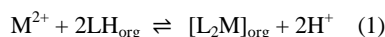
www.rsc.org/

A series of 22 tridentate unsaturated mono-anionic ligands having the atom-sequence Y-C=C-N=CH-C=C-Z¹, with Y = N, O, or S and Z = O or S, has been studied to establish whether this backbone could be used to develop strong solvent extractants for nickel(II) which will preferably also show a high selectivity over iron(III) in the pH-dependent process: 2LH_{org} + NiSO₄ ⇌ [(L)₂Ni]_{org} + H₂SO₄. All are capable of forming octahedral [(L)₂Ni] complexes with a *mer*-arrangement of the YNZ¹ donor set. X-ray crystal structures of three salicylaldimine proligands derived from 3-bromo-5-*t*-butyl-2-hydroxybenzaldehyde show these to have pre-organised donor sets in which the three donors are held in an approximately orthogonal arrangement by intramolecular hydrogen bonds. The tautomers observed are dependent on the nature of the Y atom and the extent to which it is favourable for this to form a bonding interaction with the acidic hydrogen atom on the salicylaldimine unit. X-ray crystal structure determinations of seven of the [(L)₂Ni] complexes show these to have significantly distorted octahedral coordination geometries which partly account for the proligands proving to be fairly weak Ni-extractants. DFT calculations show that extractant strength is dependent on a combination of the binding strength of the YNZ¹ donor set to the nickel ion and on the ease of deprotonation of the extractant. On this basis 3-nitro-4-*t*-octyl-6-(quinolin-8-imino)phenol is predicted, and is found, to be the strongest Ni-extractant. The extractants have low hydrolytic stability, reverting to their aldehyde precursors when solutions in water-immiscible solvents are contacted with aqueous acid, making them poor candidates for development as reagents for nickel recovery based on pH-swung processes of the type shown above.

Introduction

The increasing demand for nickel arising from its expanding uses in stainless steel, electroplating and rechargeable batteries¹ is providing an incentive for the mining industry to develop more efficient processes for its recovery from laterite ores as a consequence of the declining grade and the dearth of discoveries of sulfidic ores,² which are processed using conventional *pyrometallurgy*.³ Low grade nickelferrous laterite ores, which contain high concentrations of water and iron, are more abundant and can be processed by *hydrometallurgical* methods following High Pressure Acid Leaching (HPAL),⁴ but downstream recovery of metals is inefficient and is currently preceded by raising the pH to precipitate iron(III) oxyhydroxide waste.⁵ The ARFe (Anglo Research Iron) process² generates hematite as a product of commercial value and provides options for recovery of cobalt and nickel from acidic sulfate

streams. This paper considers how new solvent extractants might be designed to concentrate and separate nickel from such streams, using the pH-dependent equilibrium shown in Equation 1.



Cyanex[®] 301, a dialkylthiophosphinic acid, has been shown to be effective for the direct recovery of nickel and cobalt without pH adjustment.⁷ Due to reduced stability in the presence of oxidizing agents, Cyanex 301 must be used under an inert atmosphere in a closed system, achieved at Goro with the use of very large pulsed columns.^{8,9} The multi-branched decanoic acid, Versatic 10[®], has been tested extensively for nickel recovery from laterite streams but is a weak extractant,¹⁰ requiring several contacts with pH-adjustment to displace the equilibrium shown in Equation 1.[‡] It also has a high solubility in aqueous streams, requiring an additional extractant-recovery step.¹¹ The use of synergistic combinations of an organic acid and a neutral extractant has been shown to enhance the efficiency of nickel recovery greatly, but so far none of these have been implemented in commercial operations.¹² One of the best understood synergistic systems contains a mixture of a carboxylic acid such as Versatic 10[®] and

^a EaStCHEM School of Chemistry, University of Edinburgh, David Brewster Road, Edinburgh, Scotland EH9 3FJ.

^b Cytec Industries, 1937 West Main Street, Stamford, Connecticut, United States, 06902

[†] Corresponding author.

Electronic Supplementary Information (ESI) available: [details of any supplementary information available should be included here]. See DOI: 10.1039/x0xx00000x

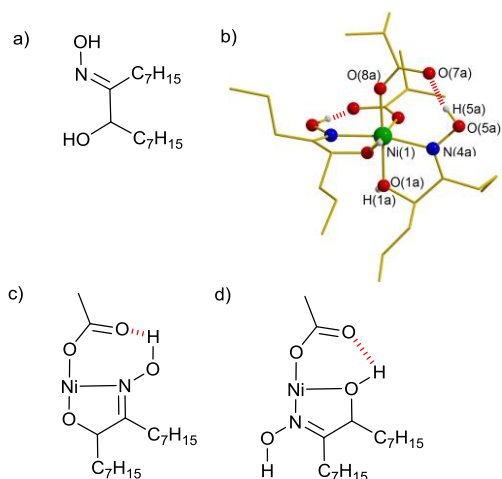


Figure 1: The structure of LIX63 (a); the X-ray crystal structure of $[\text{Ni}(\text{Pr-hydroxyoxime})_2]_2(\text{Pr-COOH})_2$ (b);¹³ the 7/5 membered ring H-bonding arrangement observed in $[\text{Ni}(\text{Pr-hydroxyoxime})_2]_2(\text{Pr-COOH})_2$ (c); and the alternative 5/6 membered ring arrangement (d).

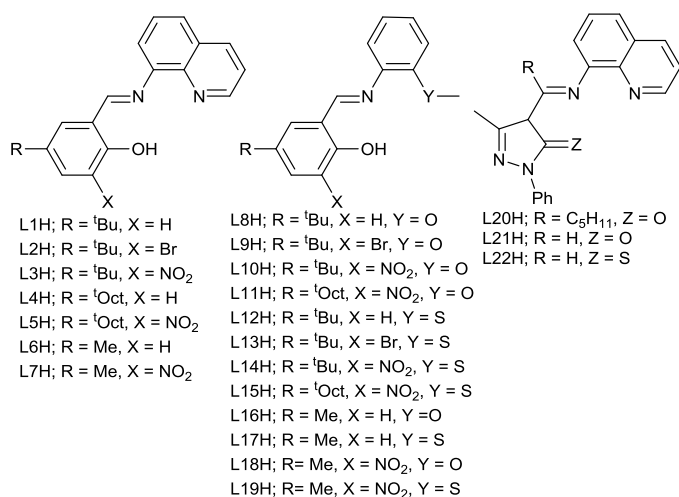


Figure 2: Tridentate salicylaldehyde (L1H-L19H), acylpyrazoloneimine (L20H and L21H) and acyl thiopyrazoloneimine (L22H) proligands.

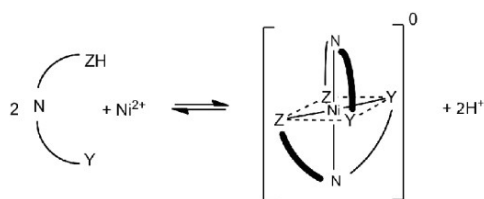
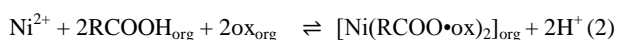


Figure 3: The formation of a neutral octahedral nickel(II) complex by *mer*-forms of the monoanionic tridentate ligands formed by deprotonation of L1H - L22H.

an α -hydroxyoxime, such as LIX 63[®] (see Figure 1).¹⁴ The extraction equilibrium is thought to involve the deprotonation of the carboxylic acid, rather than the hydroxyoxime as in Equation 2.



An X-ray structure of the model system shown in Figure 1b,¹³ contains a *pseudo*octahedral, charge-neutral, nickel complex

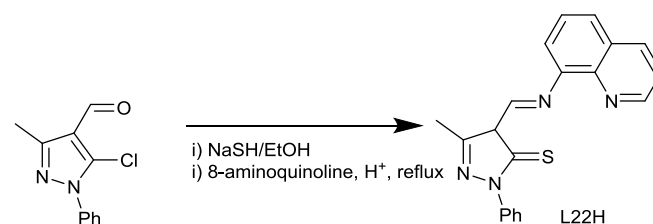
with two carboxylate and two neutral hydroxyoxime ligands. Hydrogen bonding between the ligands generates a planar *pseudo*-tridentate $[\text{NO}_2]^-$ donor set which forms a sequence of 5/7-membered chelate rings (Figure 1c). The N-OH group of the oxime unit acts as a hydrogen bond donor to the carboxylate rather than the α -hydroxy (C-OH) group which would give the 5/6-membered chelate ring sequence shown in Figure 1d.

This paper considers whether single hydrophobic ligand molecules with comparable tridentate donor sets can generate sufficiently stable and soluble complexes to extract nickel from more acidic solutions than the LIX 63/Versatic system. The salicylaldimines, L1H-L19H, and the acylpyrazolone- and acylthiopyrazolone-imines L20H-L22H shown in Figure 2 were selected for testing as these should all be readily deprotonated to give bis *mer*-Ni²⁺-complexes with approximately planar YNZ⁻ donor sets favoured by the conjugation in the ligands (Figure 3). If extractants of this type were to be used to recover nickel efficiently from laterite leach streams it would be very beneficial if they were able to transport nickel selectively into the organic phase, rejecting iron, because this would remove the need for precipitation of the latter. In the presence of iron(III) extractants should give cationic $[\text{FeL}_2]^+$ complexes, of the type characterised by Brashoveanu *et. al.*,¹⁵ that will require a counterion to balance the charge on the complex. Such salts are likely to have low solubility in the hydrocarbon diluents used in solvent extraction and this will result in preferential recovery of nickel(II) over iron(III).

Results and discussion

Synthesis and characterization of the proligands

Three 3-substituted-5-*tert*-butyl-salicylaldehyde precursors¹⁶ (**2-4**; for structures see supplementary information) for L1H-L3H, L8H-L10H and L12H-L14H were condensed with 8-aminoquinoline or with 2-methoxyaniline or 2-thiomethoxyaniline to yield the proligands. Two 3-substituted-5-*tert*-octyl-salicylaldehyde precursors¹⁶ (**5** and **6**) were used to prepare L4H, L5H, L11H and L15H in an attempt to enhance the solubility of the extractants and their nickel(II) complex. The acylpyrazolone imines L20H and L21H were obtained from similar Schiff base condensations using 1-phenyl-3-methyl-5-oxo-4,5-dihydro-1H-pyrazole-4-carbaldehyde (**1**) or 4-hexanoyl-3-methyl-1-phenyl-4,5-dihydro-1H-pyrazol-5-one (**7**). L22H was obtained by the two step, one pot, reaction of 1-(5-chloro-3-methyl-1-phenyl-4,5-dihydro-1H-pyrazol-4-yl)ethan-1-one shown in Scheme 1 using conditions developed by Smith *et al.*¹⁷



Scheme 1: The one-pot synthesis of L22H.

Proligand structures

The conjugation through the imine moiety and intramolecular hydrogen bonding in the salicylaldehyde (Fig. 4a) and the acylpyrazoloneimine prolignands (Fig. 4b) was expected to favour the pre-organisation of the donor atoms to generate a planar 6/5 chelate sequence. The extent to which the resulting donor set is orthogonal is important if the ligands are to define a regular octahedral geometry about a nickel(II) ion.

Data presented in Table 1 define the geometries of the preorganised donor atoms in the crystal structures of L2H, L9H and L13H. The structure of L9H has three crystallographically independent molecules per asymmetric unit (Figure 5). Molecule **b** is the most nearly planar with the linking carbon atoms showing ≤ 0.04 Å deviations from the plane defined by the Y1-N4-Z8 donor set of the prolignand. Molecules **a** and **c** are less planar with larger (maximum) deviations of the linking carbon atoms from the Y1-N4-Z8 plane of 0.85 and 0.65 Å respectively, and have similar conformations with the five- and six-membered potential chelating units being displaced to opposite sides of the Y1-N4-Z8 plane. The phenolic imine N4-C5-C6-C7-Z8 units show a larger inclination from this plane (25 and 40° in molecules **a** and **c**) than the methoxy imine N4-C3-C2-Y1 units for which the least squares planes are inclined by 16 and 27°. A difference map calculated during the solution of the structure of L9H indicated that the acidic hydrogen atom in molecule **b** is disordered between the phenolic oxygen, O(8b), and the imine nitrogen, N(4b), and refinement showed a 7 : 3 occupancy of these sites which correspond to the tautomers shown at the bottom of Figure 5. The solid state structures of L2H and L13H both contain two crystallographically independent molecules per unit cell. Only molecules **a** are shown in Figure 6. Inter-molecular contact distances are listed in Table 2. The thioether-substituted prolignand, L13H, exists exclusively as the conventional phenolic imine whereas L2H has the acidic hydrogen atom attached to N4 where it can form comparably strong hydrogen bonds to the quinone oxygen and quinoline nitrogen atoms, with contact distances of 2.6 and 2.7 Å respectively. This bifurcated hydrogen bonding relationship favours a highly planar conformation of the prolignand. The linking carbon atoms show smaller deviations from the Y1-N4-Z8 plane (≤ 0.35 Å) than in L9H. L13H shows very weak hydrogen bonding between the phenolic protons and the sulfur atoms of the thioether groups with long contacts (ca. 3.4 Å). The crystal structures of the prolignands suggest that the quinoline-containing L2H has the most nearly planar preorganised (*mer*) arrangement of donor atoms as judged by the angles and distances listed in Table 1.

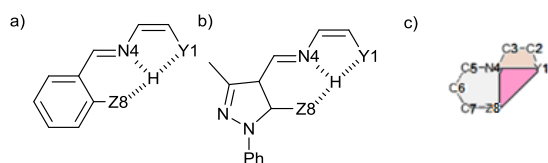


Figure 4: Salicylaldehyde and acylpyrazoloneimine prolignand structures (a and b) with approximately orthogonal Z8, N4 and Y1 donor atoms, using the atom labelling in X-ray

structure determinations below and (c) the Y1-N4-Z8 plane, and the Y1-C2-C3-N4 and N4-C5-C6-C7-Z8 least squares planes used in structure analysis (Table 1).

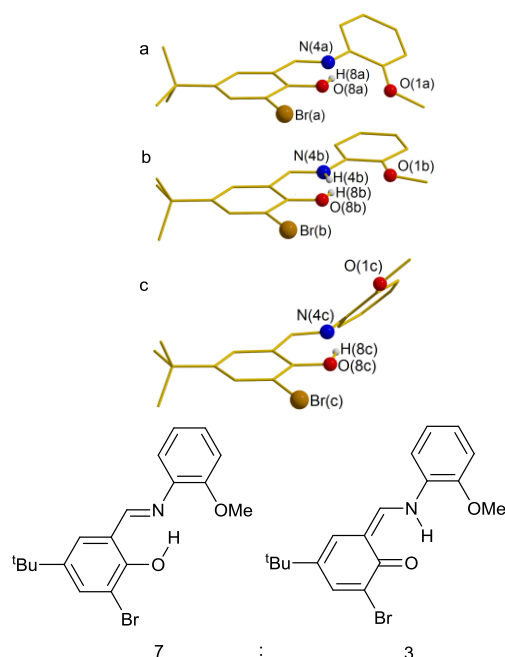


Figure 5: The structures of the three crystallographically independent molecules of L9H, a-c. Disorder of the acidic protons H(8) and H(4) in the molecule b corresponds to a 7:3 occupancy of the phenol/quinone tautomers shown.

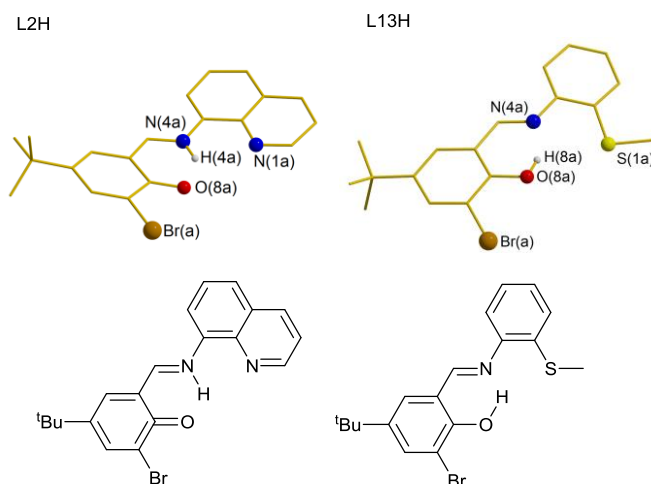


Figure 6: The X-ray crystal structures of L2H and L13H.

Nickel complex structures

The atom labelling scheme for the X-ray crystal structures of [(L2)₂Ni], [(L3)₂Ni], [(L9)₂Ni], [(L10)₂Ni], [(L13)₂Ni], [(L14)₂Ni] and [(L22)₂Ni] is shown in Figures 4 and 7. All contain two monoanionic ligands with *mer* arrangements of the tridentate [Y1-N4-Z8]⁻ donor sets, where Z = O or S, and Y = O or N or S. A comparison of the distorted octahedral geometries is provided in Table 3. The salicylaldehyde nickel complexes (see for example [(L2)₂Ni] and [(L9)₂Ni] in Figure 7) have intra-ligand *cis*-angles in the range 75.05 to 83.76° for their 5-membered chelating units and 87.76 to 96.54° for their 6-membered

ARTICLE

Journal Name

chelates. The *trans*-angles range between 161.02 and 171.30° and the angles (α) between the Y1-N4-Z8 planes vary between 87.47 and 89.21°. Intra-ligand *trans*-angles in the thiopyrazolone complex [(L22)₂Ni] (see Figure 7) and

Table 1: A comparison of the geometries of the Br-substituted salicylaldimine proligands, L2H, L9H and L13H.

Ligand	L2H (Y = N, Z = O)		L9H (Y = O, Z = O)			L13H (Y = S, Z = O)	
	a	b	a	b	c	a	b
Angles/ $^{\circ}$ between donor atoms and Z8-Y1 midpoint (H) ^a							
Y1 – M – N8	91.84	92.12	91.36	91.12	91.36	95.16	95.86
Z8 – M – N4	88.16	87.88	88.64	88.88	88.64	84.39	84.14
Y1 – N4 – Z8	84.70	83.30	95.34	79.79	95.84	77.61	78.17
Angle/ $^{\circ}$ Between the Z, N8, Y and the N8, C7, C6, C1, Z least squares planes							
γ	10.37(5)	9.51(8)	25.07(7)	0.96(8)	39.89(8)	13.08(2)	13.93(2)
Angle/ $^{\circ}$ Between the Z, N8, Y and N8, C9, C14, Y least squares planes							
δ	3.57(6)	3.68(8)	15.85(9)	0.04(1)	26.62(1)	4.97(2)	2.64(2)
Displacement/ \AA from the Z, N8, Y least squares plane							
C7	0.255(1)	0.198(1)	0.600(2)	-0.003(1)	-0.658(2)	0.294(3)	0.358(3)
C6	0.357(1)	0.335(1)	0.858(2)	0.571(2)	-0.880(2)	0.451(3)	0.479(3)
C5	0.220(1)	0.218(1)	0.511(2)	0.326(2)	-0.470(2)	0.327(3)	0.303(3)
C3	0.052(1)	0.001(2)	-0.328(2)	-0.050(2)	0.443(2)	-0.120(4)	-0.062(3)
C2	0.102(1)	-0.002(2)	-0.350(2)	0.002(2)	0.475(2)	-0.126(4)	-0.068(3)

Table 2: Intra-molecular contact distances for the Br-substituted salicylaldimine proligands, L2H, L9H and L13.

L^2H Hydrogen bond (D...A) distances/ \AA			
N(4a)-H(4a)...O(8a)	2.603(1)	N(4b)-H(4b)...O(8b)	2.579(1)
N(4a)-H(4a)...N(1a)	2.688(1)	N(4b)-H(4b)...N(1b)	2.676(1)
L^9H Hydrogen bond (D...A) distances/ \AA			
O(8a)-H(8a)...N(4a)	2.579(2)	O(8b)-H(8b)...N(4b)	2.532(2)
O(8b)-H(8b)...O(1b)	3.280(2)	O(8c)-H(8c)...N(4c)	2.567(2)
O(8a)-H(8a)...O(1a)	3.708(2)	O(8c)-H(8c)...O(1c)	3.856(2)
L^{13H} Hydrogen bond (D...A) distances/ \AA			
O(8a)-H(8a)...N(4a)	2.566(4)	O(8a)-H(8a)...S(1a)	3.384(3)
O(8b)-H(8b)...N(4b)	2.575(4)	O(8b)-H(8b)...S(1b)	3.444(3)

[[L22]₂Ni], and the pseudo-tridentate complex, [Ni(^{Pr}-hydroxyoxime)₂(^{Pr}-COOH)₂] b) in Figure 1, are closer to 180° (between 176.55 and 177.71°).

Distortion of the ligands from planarity will adversely affect conjugation and decrease the stability of their nickel complexes. Planarity can be compared using the angle, β , between the least squares planes of the 5-membered (Ni-Y1-C2-C3-N4) and 6-membered (Ni-N4-C5-C6-C7-Z8) chelate rings. The complexes of L2H, L3H and L22H, which contain iminoquinoline units, have the most nearly flat *mer*-planes with β values between 5.24 and 11.14°. In Table 3 the angle γ , between the least squares plane of N4-C5-C6-C7-Z8 and the plane of the three donor atoms, measures the deviation of the phenolic/thiopyrazolone moiety from the donor plane and δ is the angle between the least squares planes of the imine moiety, Y1-C2-C3-N4, and the donor atoms, Y1-N4-Z8.

Deviation from regular octahedral geometry will also result from variation of the donor atoms Y and Z. The thioether (Y1 = S) bonds to nickel are longer (2.41-2.49 Å) than those from the quinoline (Y1 = N) and methoxy (Y1 = O) groups (2.08-2.14 and 2.17-2.21 Å respectively), leading to [[L13]₂Ni] and [[L14]₂Ni] having smaller bite angles in their 6-membered chelate rings (N4-Ni1-Z8 falls in the range 87.76-88.76°) than in the other salicylaldimine complexes. This forces the phenolic moiety to twist out of the plane of the donor atoms (γ is between 31.08 and 36.93°). There are no unusual features associated with

the packing of the complexes in the solid state structures or with the inclusion of solvent molecules in the lattices. Further information is provided in the supplementary material,...

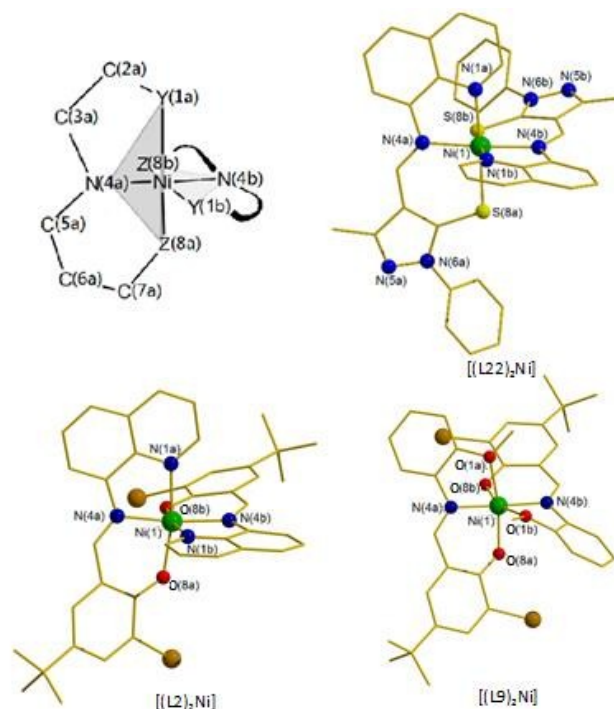




Figure 7: Atom labelling system for nickel(II) complexes with two monoanionic ligands *a* and *b* coordinating via donor atoms Y1, N4 and Z8 which have linking carbon atoms (C2 and C3 and C5, C6 and C7) and the X-ray crystal structures of [(L22)₂Ni] (top right), [(L2)₂Ni] (bottom left) and [(L9)₂Ni] (bottom right).

The crystal structures of the nickel(II) complexes provide information on the geometry around the nickel(II) cation and conformation of the ligands. Deviations from regular octahedral geometry, as determined by the bond angle variance (σ_{oct})¹⁸ according to Equation 3, and distortion of the ligands from a planar arrangement with the consequent loss of conjugation are expected to lower the stability of the complexes of the different extractants.

$$\sigma_{\text{oct}} = \sum_{i=1}^{12} (\sigma_i - 90)^2 \quad (3)$$

The quinoline-containing complexes [(L1)₂Ni], [(L2)₂Ni] and [(L22)₂Ni] have the most nearly planar ligands and the most nearly regular octahedral geometry around the nickel(II) centre as judged by the values listed in Table 3. On this basis the reagents containing this moiety and solubilising alkyl groups, L4H, L5H and L20H, may be expected to extractant nickel from more acidic solutions because they are likely to generate more stable complexes.

Table 3 A comparison of the coordination geometries of the salicylyaldimine and pyrazolone imine nickel complexes.

Structure	[[L2] ₂ Ni] (Y = N, Z = O)				[[L3] ₂ Ni] (Y = N, Z = O)		[[L9] ₂ Ni] (Y = O, Z = O)	[[L10] ₂ Ni] (Y = O, Z = O)		[[L13] ₂ Ni] (Y = S, Z = O)		[[L14] ₂ Ni] (Y = S, Z = O)		[[L22] ₂ Ni] (Y = N, Z = S)		[Ni(^{Pr} -hydroxyoxime) ₂ (^{Pr} -COOH) ₂] ¹³ (Y = O, Z = O)		
	a	B	a ^b	b ^b	A	B	a ≡ b ^c	A	b	A	b	a	b	a	b	a	b	
Bond lengths/Å																		
Ni-Y	2.089(2)	2.114(2)	2.107(2)	2.146(2)	2.091(1)	2.091(1)	2.216(2)	2.181(2)	2.177(2)	2.491(1)	2.412(1)	2.453(1)	2.425(1)	2.091(2)	2.084(2)	2.032(2)	2.026(1)	
Ni-N8	2.030(2)	2.040(2)	2.030(2)	2.027(2)	2.038(2)	2.041(2)	2.015(2)	2.004(2)	2.006(3)	2.031(2)	2.041(2)	2.027(2)	2.025(2)	2.080(2)	2.079(2)	2.061(2)	2.057(2)	
Ni-Z	2.024(1)	2.047(1)	2.046(1)	2.068(1)	2.054(1)	2.053(1)	1.964(1)	1.988(2)	1.984(2)	2.017(2)	1.988(2)	2.020(3)	1.989(2)	2.385(1)	2.370(2)	2.076(2)	2.083(2)	
Interatomic bond angles/°																		
Y-Ni-N8	80.84(7)	80.23(7)	79.97(7)	79.55(7)	80.47(6)	80.49(6)	75.05(7)	77.89(10)	77.89(10)	81.95(7)	83.76(7)	82.90(9)	83.52(6)	80.29(6)	80.72(6)	104.65(7)	103.93(7)	
N8-Ni-Z	90.45(7)	90.06(7)	90.04(6)	90.28(6)	89.97(6)	89.98(6)	90.92(7)	92.93(10)	95.95(10)	87.83(9)	88.76(9)	87.76(10)	87.96(8)	96.32(4)	96.54(5)	76.96(7)	77.04(7)	
Y-Ni-Z	171.30(7)	167.66(7)	169.86(6)	169.76(6)	170.43(6)	170.46(6)	161.02(6)	166.48(9)	164.46(9)	169.69(6)	171.02(7)	170.29(5)	170.65(6)	176.55(5)	177.20(5)	177.71(7)	177.15(7)	
Octahedral distortion factor^a																		
σ _{oct}	6.1		5.5		4.8		9.6		7.6		5.1		5.0		5.8		7.7	
Angle/° between the two Y1-N4-Z8 planes																		
α	89.19(11)		88.35(11)		89.10(9)		89.21(11)		87.47(16)		88.23(13)		87.52(13)		88.02(8)		89.03(9)	
Angle/° between the Y1-C2-C3-N4-Ni and N4-C5-C6-C7-Z8-Ni least squares planes																		
β	9.48(9)	9.02(8)	8.14(8)	11.14(8)	6.90(7)	6.92(7)	21.95(8)	7.85(12)	16.50(12)	27.52(10)	23.01(10)	26.29(8)	24.86(12)	5.24(6)	10.33(7)	3.6(2)	8.4(2)	
Angle/° between the Y1-N4-Z8 plane and the N4-C5-C6-C7-Z8 least squares plane																		
	9.21(11)	14.69(11)	12.32(11)	16.46(11)	10.57(9)	10.48(9)	26.59(11)	8.12(16)	19.95(16)	36.93(13)	31.08(14)	36.24(12)	32.26(16)	13.83(8)	1.39(8)	1.69(12)	9.12(13)	
Angle/° between the Y1-N4-Z8 plane and the Y1-C2-C3-N4 least squares plane																		
δ	4.52(13)	3.49(14)	2.63(13)	1.33(12)	1.40(11)	1.59(11)	21.17(13)	6.60(19)	13.27(19)	23.25(14)	21.25(15)	20.92(12)	24.29(18)	8.85(11)	7.87(10)	6.1(3)	12.3(3)	

^a The bond angle variance, σ_{oct}¹⁸ is the average difference of the twelve *cis*-angles from the idealised value of 90° as shown in Equation 3. ^b This complex has two crystallographically independent molecules per asymmetric unit. ^c The two ligands in [[L⁹]₂Ni] are related by a crystallographic C2 axis through the Ni atom.

Solvent extraction studies

A strong extractant will displace the pH-dependent equilibrium in Equation 1 to favour the formation [L₂Ni], leading to nickel(II) extraction into the organic phase at a lower pH. Plots showing the pH-dependence of nickel(II) uptake from aqueous sulfate solutions by L4H, L5H, L11H and L15H into chloroform are presented in Figure 8. No appreciable nickel extraction was detected below pH 2 and loading of the organic phase to a theoretical nickel maximum value, assuming the 1:2 (metal:ligand) ratio in the extracted [L₂Ni] species, could not be achieved at pH ≥ 4.5 because nickel hydroxides were precipitated. L15H and L11H are too weak to obtain a value for pH_{0.5} (the pH at which 50% of the theoretical loading is achieved), but it is possible to define

the order of extractant strength as: L5H > L4H > L15H > L11H. L5H and L4H have identical N₂O⁻ donor sets but the incorporation of a nitro group *ortho* into the phenol moiety in L5H increases the extractant strength by one pH unit based on pH_{0.5} values, which correspond to approximately to an order of magnitude increase in the extraction distribution coefficient. The origin of this is discussed below. L15H and L11H also have nitro groups *ortho* to the phenol OH group but different Y donor atoms, a thioether and an ether. The NSO⁻ donor set of L15H can load nickel into the organic phase at a lower pH than L11H, which has a NO₂⁻ donor set, but both are significantly weaker than the quinoline containing reagents, L4H and L5H.

Imine extractants have low stability under acidic conditions and readily hydrolyse to form their component aldehydes and amines.¹⁹ The low hydrolytic stability of the

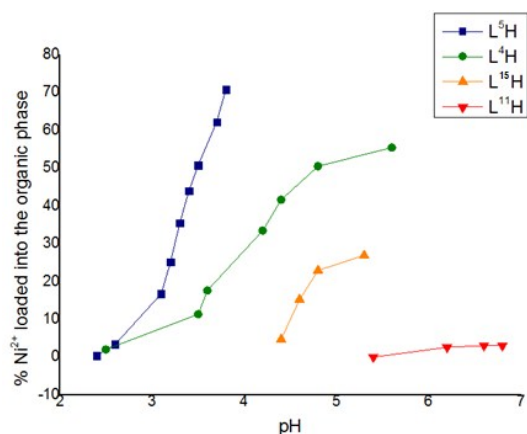


Figure 8: The pH-dependence of nickel-loading by 0.005 M CHCl_3 solutions of L4H, L5H, L11H and L15H from an equal volume of aqueous 0.01 M NiSO_4 . 100% loading is equivalent to that expected for formation of a 1 : 2 complex $[\text{Ni}(\text{L})_2]$.

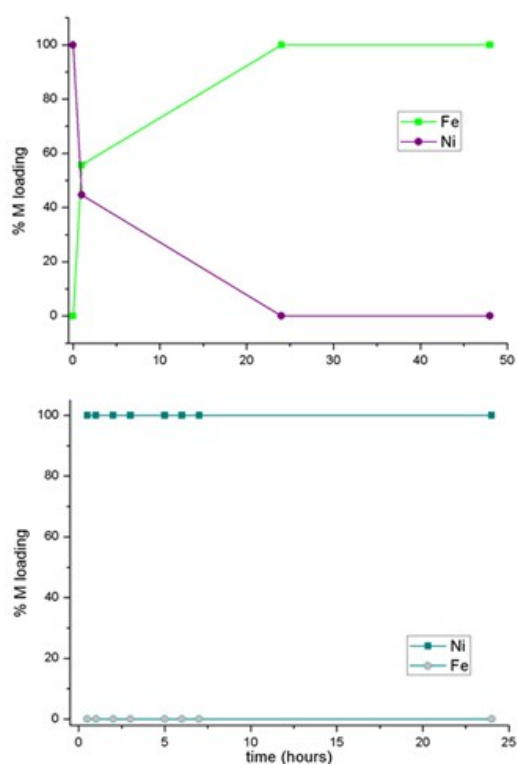


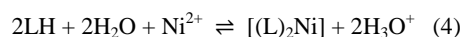
Figure 9: Loading of nickel(II) and iron(III) when 1.8 mM solutions of $[\text{NiL}_2]$ in toluene were contacted with a 1.8 mM aqueous solution of $\text{Fe}_2(\text{SO}_4)_3$ (L²⁰ top, L²² bottom). The % metal loading is based on the ligand available in toluene forming $[\text{Ni}(\text{L})_2]$ or $[\text{Fe}(\text{L})_3]$ complexes.

pyrazolone imine reagents L20H-L22H prohibited conventional studies of the pH dependence of metal-loading as in Figure 8. Nevertheless, the binding preference for uptake of nickel(II) or iron(III) by the pyrazolone imine reagents could be investigated by mixing a toluene solution of preformed $[(\text{L})_2\text{Ni}]$ with aqueous $\text{Fe}_2(\text{SO}_4)_3$ (see Figure 9). ICP-OES analysis of $[(\text{L}20)_2\text{Ni}]$ solutions showed that nickel transferred to the aqueous phase and iron was taken up by the toluene solution. ^{13}C NMR analysis of the concentrated organic phase showed that extractant L20H had been

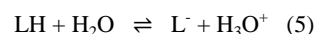
hydrolysed to the parent acylpyrazolone. Formation of the charge neutral $[(\text{acylpyrazolonate})_3\text{Fe}]$ complex is presumably favoured because the hard iron(III) ion is provided with an O_6^{3-} donor set. The thiopyrazolone complex $[(\text{L}22)_2\text{Ni}]$ was stable under similar conditions and no iron was transported into the organic phase (Figure 9). Soft sulfur donor atoms provide a less favourable donor set for iron(III) and the formation of $[(\text{L})_3\text{Fe}]$ *via* hydrolysis of the imine can be assumed to be less thermodynamically favourable.

Computational Studies

Previous work has shown that calculated (gas phase) enthalpies of formation, ΔE_f , for copper complexes formed by a series of phenolic oximes correlate with their measured strengths as solvent extractants.²⁰ The energies of the energy-minimised structures of the proligands L6H, L7H, L16H-L19H, the related ligands (L) and their complexes, $[\text{L}_2\text{Ni}]$, were calculated (see ESI) and used to evaluate the formation enthalpy (ΔE_f) associated with the process in Equation 4.



To define the origins of the dependence of the variations of formation enthalpies on the nature of the proligands, the deprotonation enthalpies (ΔE_d) for the reaction in Equation 5 were calculated using Equation 6,



$$\Delta E_d = [\text{L}^-(E_{\text{tot}}) + \text{H}_3\text{O}^+(E_{\text{tot}})] - [\text{LH}(E_{\text{tot}}) + \text{H}_2\text{O}(E_{\text{tot}})] \quad (6)$$

and binding enthalpies (ΔE_b), the energy released in bringing together two preformed anions, L^- , and a Ni^{2+} cation in the gas phase were calculated using the terms in Equation 7;

$$\Delta E_b = [\text{Ni}_{\text{complex}}(E_{\text{tot}})] - [\text{L}^-(E_{\text{tot}}) + \text{Ni}_{\text{cation}}(E_{\text{tot}})] + \text{BSSE} - 2\text{RT} \quad (7)$$

In Equations 6 and 7 E_{tot} is made up of the sum of the electronic (E_{el}), vibrational (E_{vib}), rotational (E_{rot}) and translational (E_{trans}) energies as shown in Equation 8.

$$E_{\text{tot}} = E_{\text{el}} + E_{\text{vib}} + E_{\text{rot}} + E_{\text{trans}} \quad (8)$$

The phenolic tautomer of L6H was shown to be 13 kJ mol^{-1} lower in energy than the quinone in the gas-phase, and a similar trend was established for the other salicylaldimines. The nickel(II) binding energies (ΔE_b) and proligand deprotonation energies (ΔE_d) were separately calculated, according to Equations 6 and 7, to determine how structural variations of the ligand affect these processes. An analysis of the energy terms in Table 4 provides an insight into the origins of the variations in formation energies of complexes in the gas phase which correlate with measured strengths of the extractant analogues (see below).

For the nitro-substituted ligands L7H, L18H and L19H, values of the calculated formation energies, ΔE_f , follow the

trend of measured extractant strengths of the t-octyl homologues (see Figure 8). Extractant strength varies with the nature of the donor set in the order $\text{N}_2\text{O}^- > \text{NSO}^- > \text{NO}_2^-$. The calculated deprotonation energy (ΔE_d) is more favourable for the nitro-substituted proligand, L7H, than for the unsubstituted analogue, L6H, by 61 kJ mol^{-1} . A similar trend was found for the other nitro-substituted proligands, L18H and L19H. Conversely, the nickel(II)-binding energies, ΔE_b , of the anionic forms of L6H, L16H and L17H are more favourable than their nitro-analogues (Table 4). This is consistent with the electron withdrawing nitro group increasing the acidity of the reagents whilst decreasing the basicity of their conjugate anions.

Table 4: Formation energies, ΔE_f , binding energies, ΔE_b , and deprotonation energies, ΔE_d , for proligands L⁴H, L⁵H and L¹⁶⁻¹⁹H calculated using B3LYP/6-31G(d,p).

Proligand	ΔE_f (kJ/mol)	ΔE_d (kJ/mol)	ΔE_b (kJ/mol)
L6H (X = H and Y = N)	-1279	784	-3066
L16H (X = H and Y = O)	-1219	793	-3028
L17H (X = H and Y = S)	-1209	778	-2773
L7H (X = NO ₂ and Y = N)	-1315	723	-2769
L18H (X = NO ₂ and Y = O)	-1243	729	-2710
L19H (X = NO ₂ and Y = S)	-1259	715	-2696

The low deprotonation energy of the thioether appears to arise from the sulfur not being able to form an effective intramolecular hydrogen bond with the phenolic hydrogen, making it easier for the latter to be released. The absence of an intramolecular thioether to phenolic hydrogen interaction is observed in the solid state structure of L13H, contrasting with the structure of the ether analogue L9H (molecule b) and the quinoline analogue L2H. Despite the thioether L19H having the lowest deprotonation energy, the formation energy of its nickel complex is much less favourable than that of the quinoline analogue L7H. This arises because the binding energy of the conjugate anion to nickel(II) is much more favourable for the latter.

Conclusion

Despite being pre-organised by intramolecular hydrogen bonding to provide nearly orthogonal YNZ⁻ donor sets, the new tridentate reagents are not strong nickel(II) extractants. X-ray structure determination has shown that they form the expected 2:1 *mer*-complexes, but with significant deviations from regular octahedral geometry. Extraction strength is very dependent on the nature of the donor set, with N-donor quinoline reagents recovering nickel at a lower pH than their *o*-methoxyphenyl and *o*-thiomethoxyphenyl analogues. The introduction of electron-withdrawing substituents onto the chelating unit containing the ionisable proton increases extractant strength, e.g. the nickel(II)-extraction coefficient of the *o*-nitro-substituted reagent, L5H, is more than an order of magnitude greater than that of the unsubstituted analogue L4H.

The donor sets provided by the quinoline-containing reagents have slightly smaller angular distortions from regular octahedral geometry than those in the model complex $[\text{Ni}(\text{Pr-hydroxyoxime})_2(\text{Pr-COOH})_2]$, but the bond lengths to nickel(II) fall in a slightly wider range. If the regularity of the coordination geometry assumed by the nickel ion is an important criterion in defining the stability of complexes, favouring their formation in the extraction equilibrium, there are no obvious benefits provided by the new tridentate salicylaldimine reagents. The energies of formation of the nickel complexes in the gas phase, ΔE_f , evaluated by DFT calculations, show a good correlation with the measured $\text{pH}_{0.5}$ of the extractant analogues, providing further evidence that this modelling strategy is an effective tool for predicting the strength of cation exchange extractants and assessing the different effects of varying a substituent in a series of analogous compounds.

Because the calculations do not attempt to take account of solvation energies, the correlation between the energies of gas phase equilibria and those of equilibria involving two solvents is at first sight surprising, but this has now been observed in several different systems.^{16,21,22} An important feature of each of these systems is that the only variable is the nature of a small substituent in a given class of extractant. The metal species removed from the aqueous phase and consequently the energy involved in hydration and dehydration of this and charge-balancing protons remain constant in a system. The small variations to substituents in the hydrophobic extractants are expected to result in minor differences in the solvation energies of complexed and uncomplexed forms of the extractants in the water-immiscible solvent. Consequently, the effects of substituents on both the ease of deprotonation of the extractant and the binding energy of the resulting anion to nickel(II) will make the major contribution to the relative strengths of a coherent series of extractants such as L4H, L5H, L11H, and L15H.

The strongest of the new extractants, the quinoline-containing reagents, would be able to operate under comparable conditions to synergistic mixtures of Versatic 10[®] and α -hydroxyoximes, i.e. at $\text{pH} > 3$, after iron(III) has been precipitated as in the Goro and Bulong processes.^{5, 23} However, the currently tested versions do not have very high solubility in hydrocarbon solvents which will limit mass-transport efficiency. Imine linkages are susceptible to hydrolysis and consequently they would decompose in continuous operations under conditions similar to those used for Ni-recovery by Versatic 10[®]/LIX63[®] mixtures.⁵

Acknowledgments

We thank the EPSRC, Anglo American and Cytec Industries for funding PhD studentships for JWR and JRT and EaStCHEM for access to the Research Computing Facility.

Notes and references

‡ Metal extraction by hydrophobic carboxylic acids often involves more complicated stoichiometries than those implied in Equation 1. When the extractant is present in excess, usually both carboxylate anions and neutral carboxylic acid molecules are coordinated to the metal ion. These arrangements allow the hydrogen bonds, which are favoured in the metal free extractant, to be retained in the supramolecular configuration of the extracted.¹¹

1. D. J. Hanson, *Chemical & Engineering News*, 2003, **81**, 82.
2. C. Biley, M. Pelsler, P. den Hoed and M. Hove, Proceedings of the 7th Southern African Base Metals Conference, Mpumalanga, South Africa 2013.
3. G. M. Mudd, *Ore Geology Reviews*, 2010, **38**, 9-26.
4. R. G. McDonald and B. I. Whittington, *Hydrometallurgy*, 2008, **91**, 35-55.
5. S. Donegan, *Minerals Engineering*, 2006, **19**, 1234-1245.
6. *WO Pat.*, WO2011015991, 2011.
7. C. Bourget, B. Jakovljevic and D. Nucciarone, *Hydrometallurgy*, 2005, **77**, 203-218.
8. K. C. Sole and J. B. Hiskey, *Hydrometallurgy*, 1992, **30**, 345-365.
9. K. G. Fisher, Proceedings of the Southern African Base Metals Conference 2011, Phalaborwa, South Africa, 2011.
10. J. S. Preston, *Hydrometallurgy*, 1985, **14**, 171-188.
11. N. N. Tanaka M, and Sasane S, *journal of Inorganic & Nuclear Chemistry*, 1969, **31**.
12. C. Cheng, K. R. Barnard, W. Zhang and D. J. Robinson, *Solvent Extraction and Ion Exchange*, 2011, **29**, 719-754.
13. K. R. Barnard, G. L. Nealon, M. I. Ogden and B. W. Skelton, *Solvent Extraction and Ion Exchange*, 2010, **28**, 778-792.
14. K. R. Barnard and N. L. Turner, *Hydrometallurgy*, 2011, **109**, 29-36.
15. A. L. Nivorozhkin, A. I. Uraev, G. I. Bondarenko, A. S. Antsyshkina, V. P. Kurbatov, A. D. Garnovskii, C. I. Turta and N. D. Brashoveanu, *Chem. Commun.*, 1997, 1711-1712.
16. R. S. Forgan, B. D. Roach, P. A. Wood, F. J. White, J. Campbell, D. K. Henderson, E. Kamenetzky, F. E. McAllister, S. Parsons, E. Pidcock, P. Richardson, R. M. Swart and P. A. Tasker, *Inorg. Chem.*, 2011, **50**, 4515-4522.
17. A. Smith, PhD, University of Edinburgh, 1999.
18. K. Robinson, G. V. Gibbs and P. H. Ribbe, *Science*, 1971, **172**, 567-570.
19. J. R. Turkington, PhD, University of Edinburgh, 2011.
20. R. S. Forgan, *Inorg. Chem.*, 2011, **50**, 4515-4522.
21. R. J. Ellis, J. Chartres, D. K. Henderson, R. Cabot, P. R. Richardson, F. J. White, M. Schroeder, J. R. Turkington, P. A. Tasker and K. C. Sole, *Chem. - Eur. J.*, 2012, **18**, 7715-7728.
22. M. R. Healy, V. A. Cocallia, E. D. Doidge, A. J. Fischmann, J. B. Love, C. A. Morrison, J. W. Roebuck, T. Sassi, P. A. Tasker, Proceedings of the International Solvent Extraction Conference, Würzburg, Germany, 2014.23. I. O. Mihaylov, E. Krause, D. F. Colton, Y. Okita, J.-P. Duterque, J.-J. Perraud, 2000, *CIM Magazine*, 93; [B. I. Whittington, D. Muir](#), *Mineral Processing and Extractive Metallurgy Review*, 2000, **21**, 527-599; D. S. Flett, *Principles and practices of solvent extraction. 2nd Edition*, Marcel Dekker, New York, **2004**, 760-762

